ISSN: 0975-8585

Research Journal of Pharmaceutical, Biological and Chemical Sciences

Study of Molecular Mobility in Textured Films of a Copolymer of Vinylidene Fluoride and Tetrafluoroethylene with Different Thermal Prehistory.

Anastasia S. Gadlevskaya*, Eugene V. Luchkin, and Ekaterina E. Kozlova.

Joint Stock Company «Federal State Research and Design Institute of Rare Metal Industry» (Institute «GIREDMET»), 119017, Moscow, Russian Federation

ABSTRACT

The processes of dielectric relaxation in the films of copolymer vinylidene tetrafluoroethylene composition 94:6, which have different original morphology. In one case, in the film discovered the spherulites, while another noted their absence. During the cold hood of these films in both cases, a decrease in crystallinity. It leads to a decrease of the activation energy for the main area of relaxation near the glass transition. For sample, where in the original film spherulites are absent, the cold hood intensifies as the main relaxation process and the mobility associated with the local dynamics. Discovered that in the case of spherulitic morphology after cold drawing in the amount of micro-cracks occur. This is accompanied by a decrease in the activation barrier of the thermal motion. During the cold extractor in the present case is more complete orientation of the lamellae along the axis of extrusion. It is interpreted from the perspective of improving anadromous intense circuits in milameline amorphous intervals.

Keywords: vinylidene fluoride, tetrafluoroethylene, copolymer, textured films, relaxation

Corresponding author

ISSN: 0975-8585

INTRODUCTION

Poly(vinylidene fruoride) (PVDF) is known to be a convenient object for studying the processes of orientation in crystallizable polymers when the phenomena of polymorphism are well pronounced [1]. In this work, we discuss a problem concerning the development of microcracks in crystallizable polymers which is important for advanced technologies [2–5]. For PVDF and related copolymers with ferroelectric properties [6], one may follow the effect of microcracks on the residual polarization of a ferroelectric [7]. In this case, due to a decrease in the dielectric permittivity, one can increase the level of the piezoelectric constant g and, thus, provide an improvement in the characteristics of piezoelectric sensors based on the above materials that are applied in various areas of science and technology [8, 9].

EXPERIMENTAL

To prepare oriented films, the initial (isotropic) samples of VDF–tetrafluoroethylene (TFE) copolymer with a composition of 94 : 6 (the fractional content of head-to-head defects is equal to 4.5 mol % [10]) were obtained by crystallization or were cast from a solution in DMF (sample 2) or its mixture with ethyl acetate (sample 1). In both cases, the orientation of the samples was accomplished by uniaxial cold stretching on an Instron-1122 tensile machine at a cross-head speed of 10 mm/min. For film 1, the temperature of tensile drawing was 60°C, whereas, for film 2, it was equal to 22°C. The longitudinal speed of sound in isotropic and oriented films was measured by the pulse method at a frequency of 200 kHz [11]; the level of flow birefringence Δn was recorded on a Berek compensator. The components of complex dielectric permittivity ε* were estimated for samples with vacuum-deposited 0.1 μm thick Al electrodes. The procedure for calculating the activation parameters of relaxation processes was described in [12].

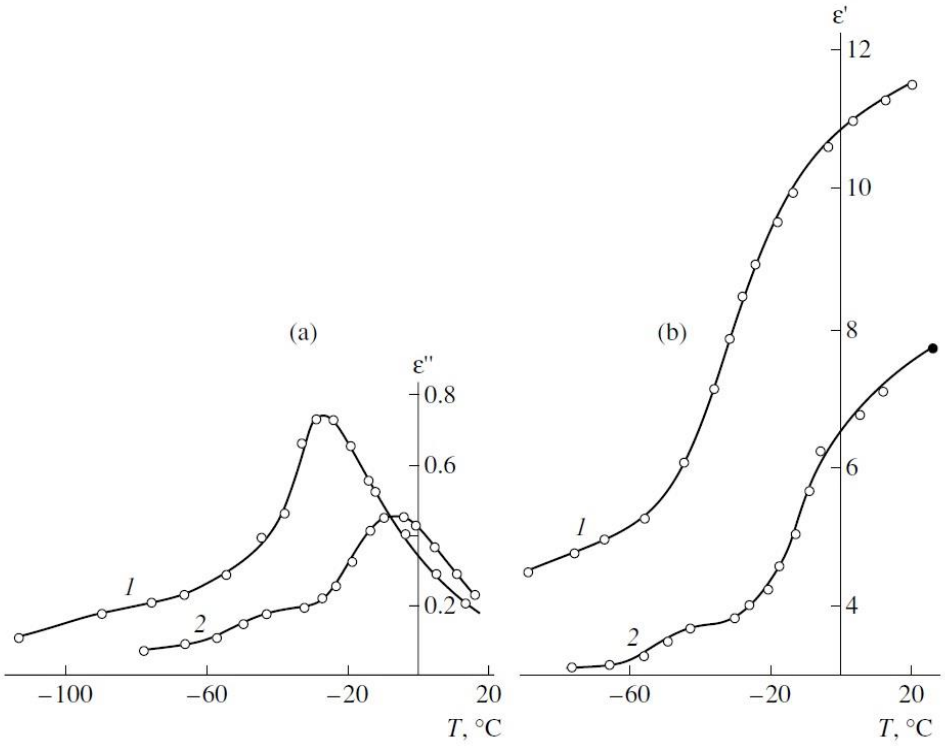

Fig. 1. Isochronic dependences of (a) variations in the loss factor and (b) dielectric permittivity for the oriented films 1 and 2. v = 1 kHz.

Isotropic and oriented films of the copolymers were characterized by the spectral dependences of light transmittance in a visible spectral region. The level of light transmittance is related to the excess light scattering through the Lambert–Berr law

ISSN: 0975-8585

$$I = I_0 \exp(-\tau d), \quad (1)$$

where I and I_0 stand for the intensities of transmitted and incident light on a film with thickness d, respectively, and τ is the specific opacity, which characterizes the excess light scattering from static fluctuations of the refractive index (local density).

RESULTS AND DISCUSSION

As was shown in [12], the above samples in their isotropic state are characterized by quite different structure and molecular mobility in the glass transition region. In this connection, it is important to investigate the character of the above dynamics for anisotropic samples under similar conditions of orientation via cold uniaxial drawing. For comparison, Fig. 1 presents the isochronic dependences of the components of ε* for the oriented samples 1 and 2. The temperature position of the ε'' maxima suggests that, as compared with sample 2, the relaxation processes in sample 1 are shifted to lower temperatures. This trend is also illustrated in the relaxation maps shown in Fig. 2. In the case of both isotropic and oriented films, the above dependences, as presented in the Arrhenius coordinates, appear as two intersecting straight lines. The low-temperature part of such dependences is associated with the microbrownian cooperative α_a-relaxation process provided by glass transition. The region of higher temperature mobility is attributed to the appearance of complex (experimentally unresolved) α_a -relaxation and a more localized β-process [12]. As follows from Fig. 2, upon tensile drawing, the frequencies of reorientation in film 1 increase, whereas, on the contrary, in the case of film 2, the above values tend to decrease. Figure 3 shows quite similar changes in the character of the temperature dependences of absorption intensities $\Delta\varepsilon = \varepsilon_0 - \varepsilon_\infty$, where ε_0 and ε_∞ stand for the static and high-frequency dielectric permittivity, respectively; the latter values are estimated from the ε''– ε' diagrams on the complex plane. The orientation of film 1 is accompanied by a marked increase in the Δε values, whereas, on the contrary, in the case of film 2, the corresponding values tend to decrease. Table 1 presents the parameters of activation processes. As is seen, upon tensile drawing, the glass transition temperature of film 2 increases. This trend is usually observed for the orientation of crystallizable polymers [13–16]. For the oriented film 1, a decrease in T_g and in the conditional freezing temperature of the complex dispersion α_a-β-region attests that the cold drawing assists enhancement of the molecular mobility. This behavior seems to be rather unexpected even though, recently, a quite similar process of “stress-induced softening” was observed for some glassy polymers [17].

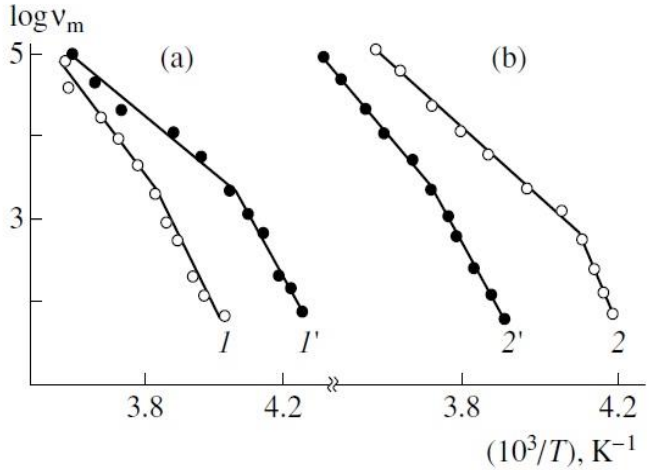

Fig. 2. Relaxation maps for (*1*, *2*) isotropic and (*1*', *2*') oriented films (a) 1 and (b) 2.

Therefore, the cold drawing of films 1 and 2 is characterized by quite different changes in the dynamics. In this connection, a further analysis is focused on finding differences in the structural parameters as developed upon the orientation of the above films. Figure 4 shows the SAXS curves as recorded in the meridional direction for both drawn films [18, 19]. As is seen, film 1 is characterized by a curve with a maximum, which is typical of crystallizable polymers, and this profile attests to the development of a long

ISSN: 0975-8585

period. For film 2, this maximum escapes any detection due to a marked increase in intensity at small angles. The analysis of two-dimensional X-ray scattering patterns [20] suggests the development of ellipsoidal microcracks in the oriented film 2 and that the long axis of the above microcracks is aligned along the direction of tensile drawing. Figure 4 presents the data as plotted in the Guinier coordinates [19]. As is seen, the scattering sites (microcracks) are characterized by a wide size distribution. This fact implies that some microcracks are also capable of visible light scattering. Figure 5 supports the above conclusion, because the specific opacity of the oriented film 2 appears to be much higher than that in film 1. The regions of microcracks are characterized by a reduced local density and, hence, the oriented film 2 shows a decreased dielectric permittivity (Fig. 1).

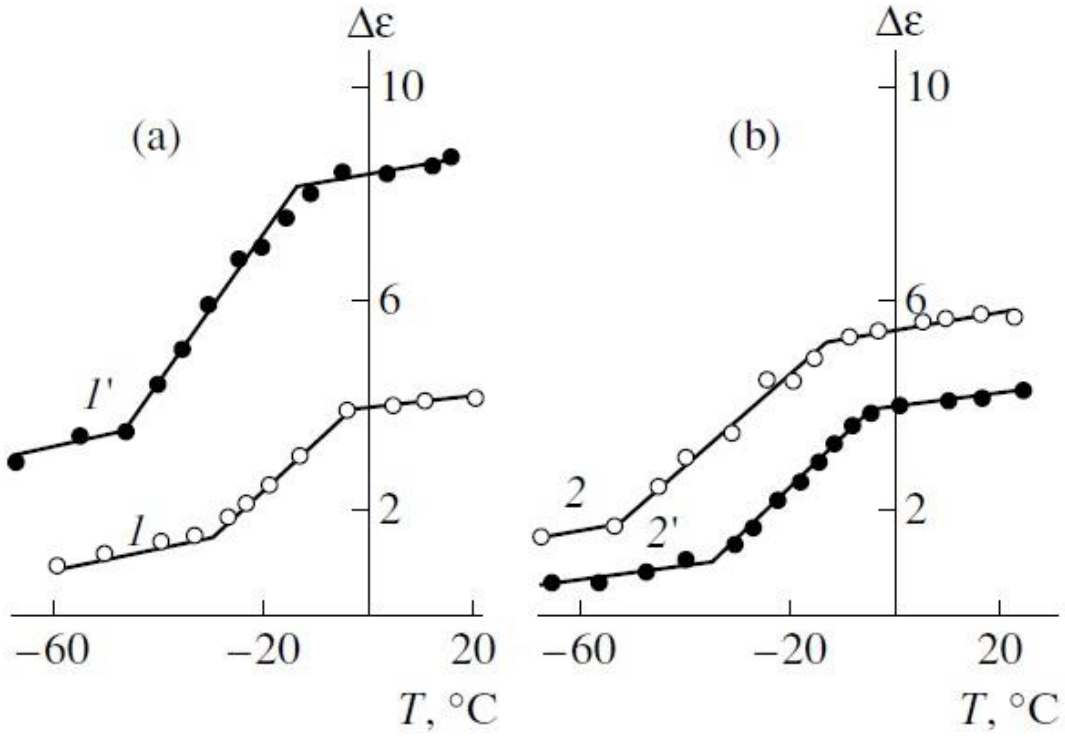

Fig. 3. Temperature dependences of the intensity of dielectric absorption for films (a) 1 and (b) 2 in (*1*, *2*) isotropic and (*1*', *2*') oriented states.

One may also discuss the reasons behind the development of microcracks upon orientation in film 2 and their absence in film 1. Film 2 is crystallized from a solution in DMF, which shows a high affinity to PVDF. In this case, spherulites with mean sizes of 2.6 μm are developed [12]. However, for sample 1 with the same sizes of crystallites (Table 1), such structures are not detected. This observation may be explained by the fact that this sample is formed upon crystallization from the DMF–ethyl acetate mixture when the former component serves as a poor solvent. In this case, the specific effects of the interaction of a PVDF chain with solvent molecules [21] markedly assist the processes of the precipitation of the polymer phase from the solution [22]. As a result, these processes prevent the development of spherulites. Different types of the formed supramolecular structures in both films may lead to changes in the microstructure of interlamellar amorphous regions. The IR spectra of both films (Fig. 6) show bands at 880, 1075, and 1177 cm^{-1} which are observed upon crystallization in any polymorphic modification [1, 23]; such modifications are insensitive to chain conformation [1].

ISSN: 0975-8585

Table 1. Activation parameters of low-temperature relaxations in isotropic and oriented films of copolymers 1 and 2

Sample	Structure	Tg, °C	ΔE	ΔH	ΔS, ent. units	T^{β}_{g}, °C	ΔE	ΔH	ΔS, ent. units
			kJ/mol				kJ/mol		
		α_a-relaxation				α_a-β-relaxation			
1	Isotropic	-34	184	181	523	-46	113	111	264
	Oriented	-48	151	149	435	-70	77	75	144
2	Isotropic	-43	188	186	586	-63	79	77	146
	Oriented	-31	158	156	417	-42	100	98	197

In film 1, the normalized optical densities of the above bands appear to be higher (Table 2). On the other hand, the fraction of isomers typical of the amorphous phase [1] is lower (Table 3). This fact implies that the crystallinity and packing density of the amorphous phase chains in the isotropic film 1 is higher than that in film 2. The values of the longitudinal speed of sound and acoustic modulus E (Table 2) for such films prove the above conclusion. Comparing curves 1 and 2 in Fig. 6 and the data in Table 3, one may conclude that, in film 1, the intensity of the band at 1235 cm^{-1} is much higher; this band is responsible for the γ-crystallographic modification with the $T_3GT_3G^-$ chain conformation [1, 19]. Therefore, in addition to the ferroelectric β-phase, the above isotropic films also contain the formed crystals of the γ-phase but, in film 1, its fractional content appears to be higher. Since the γ-phase is characterized by a lower packing density as compared with that of the β-form [1], this should lead to a decrease in the macroscopic density. The fact that both initial films 1 and 2 are characterized by similar densities (Table 1) does not diminish the validity of the conclusion concerning different degrees of crystallinity and packing densities in the amorphous regions of the films studied.

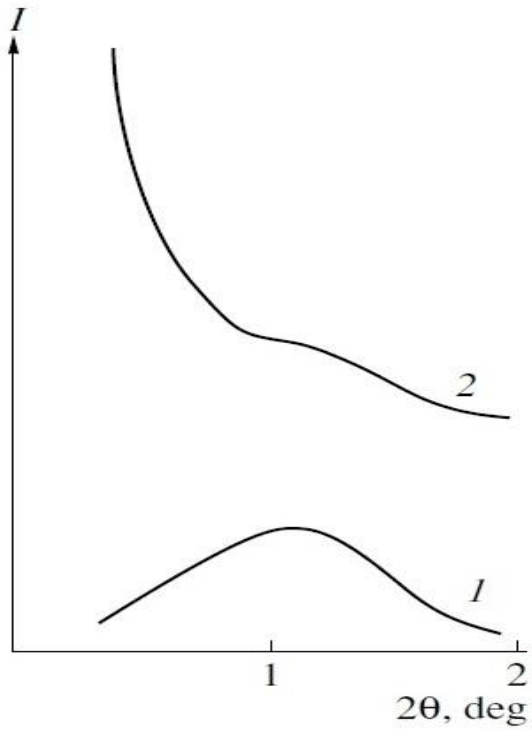

Fig. 4. Meridional SAXS reflection for the oriented films 1 and 2.

At the temperatures of cold drawing, the principal mode of thermal motion in the above isotropic materials is provided by the complex α_a-β-relaxation process (Fig. 2). As follows from Table 1, in film 1 both the enthalpy and entropy of activation of the above process appear to be much higher, attesting to a higher packing density of its amorphous phase. The above observation may explain the stress-induced development of microcracks in film 2 and their absence in film 1. As follows from the data on the Raman scattering for PE with different structures [3], the decrease in resistance to the development of microcracks is related to an

ISSN: 0975-8585

increase in the local mechanical stresses on the polymer backbone. If the development of microcracks is treated in terms of the fluctuation mechanism, the activation parameters of the molecular dynamics should assume the key role in this case. The lower the parameters, the higher the probability of the development of increased local stresses on the bond, which promotes the formation of microcracks. The lower packing density of chains in the amorphous phase of isotropic film 2 should complicate the mechanism of the stress-induced conformational rearrangements, and it is the formation of microcracks that makes this process energetically favorable.

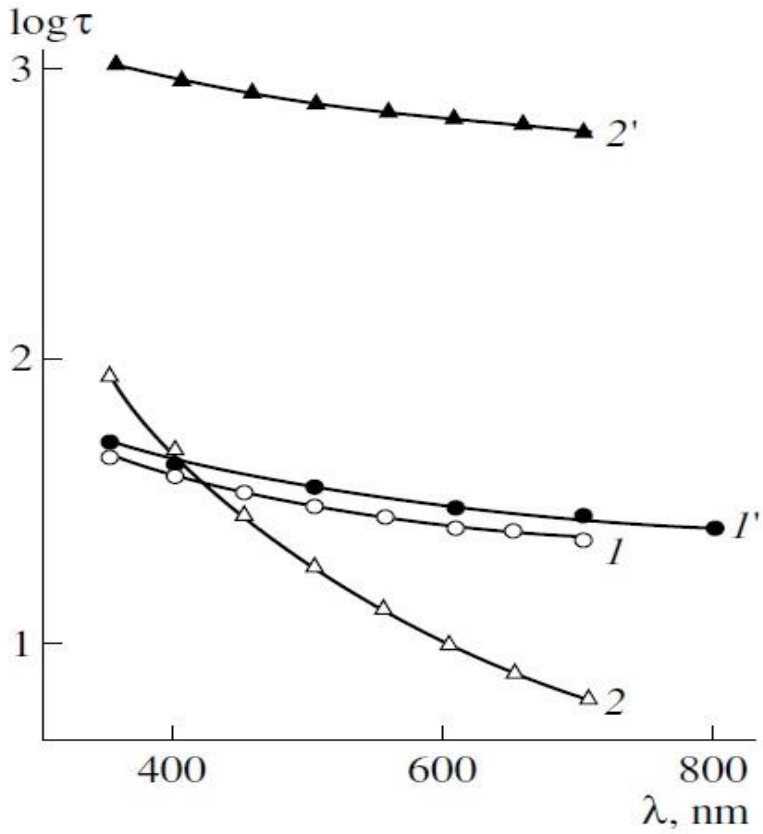

Fig. 5. Spectral changes of specific opacity in (*1*, *2*) isotropic samples and (*1*', *2*') oriented films.

Let us resort to the characteristics of the molecular mobility (Figs. 1–3, Table 1) of the oriented films. Let us first consider the results obtained for film 1. As follows from Fig. 3a, the cold drawing leads to a multifold increase in Δε for the α_a-dispersion (the temperature region above –40°C). As the material becomes anisotropic, upon the deposition of electrodes onto the film surface, we deal with the components of ε* with indices 33 when direction 3 corresponds to the plane normal to the film. If we assume that the principal contribution to the above relaxation processes is provided by the kinetic units in the plane zig-zag conformation for which the dipole moment is perpendicular to the chain axis, then [24]

$$\Delta\varepsilon = \Delta\varepsilon_{33} = \xi \frac{\pi n}{3kT}[1 + (\cos^2\theta)]\mu_{eff}^2, \qquad (2)$$

where ξ is the factor of a local field, *n* is the concentration of dipoles with the effective dipole moment μ_{eff}, and ϑ is the angle of reorientation of kinetic units with respect to the drawing axis. This angle characterizes the Hermans orientation function *f*:

$$f = [3(\cos^2\theta) - 1]/2. \qquad (3)$$

According to expression (2), with no account for ξ, an increase in Δε in film 1 upon its cold drawing may be related to changes in n, μ_{eff}, and θ. Let us demonstrate how the three parameters contribute to the above intensification of the α_a-process. As follows from Tables 3 and 4, upon the cold drawing of film 1, the

normalized intensities of the bands at 470, 490, and 510 cm^{-1} corresponding to the amorphous phase are , °e markedly increased. This fact implies that the cold drawing is accompanied by an additional amorphization of the isotropic film 1. This behavior is also proved by the temperature dependences of the speed of sound (Fig. 7) in the films studied. The value of the step in ΔC(T) as seen in the glass transition region is controlled by the fractional content of the disordered phase [25]. Comparing curves 2 and 2' shows that, as a result of cold drawing, the content of this phase increases. The above evidence allows one to draw an important conclusion. As in film 1, no development of spherulites is observed [12]; the as-formed morphology favors a far more efficient process of disassembling of lamellas upon cold drawing [26].

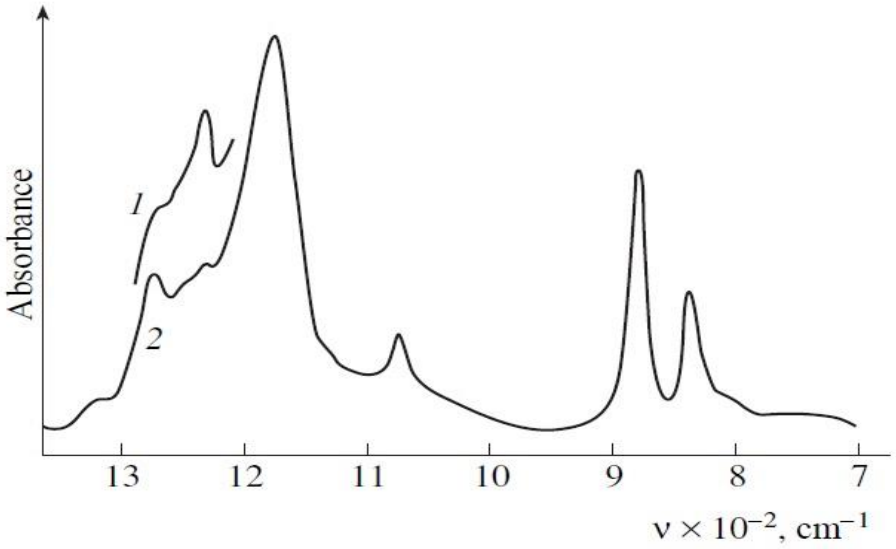

Fig. 6. IR spectra of isotropic films 1 and 2.

Therefore, the data obtained by the two independent methods unequivocally suggest an additional amorphization of isotropic films as induced by cold drawing; this corresponds to an increase in the concentration n of the kinetic units for the α_a-dispersion.

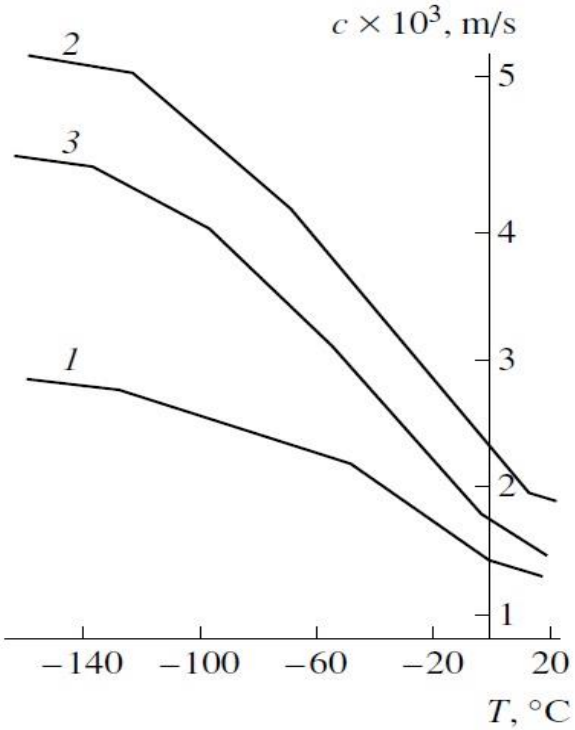

Fig. 7. Temperature dependences of the speed of sound in (*1*) isotropic film 2 and oriented films (*2*) 1 and (*3*) 2.

Taking into account the fact that, upon cold drawing, the intensities of the IR bands at 470 and 510 cm^{-1} increase (Tables 3, 4), one may expect changes in μ_{eff}. The above bands characterize the segments of the amorphous phase in the plane zig-zag conformation [1]. In the latter case, the dipole moment is perpendicular to the axes of PVDF macromolecules which are oriented along the direction of cold drawing (see *f*a in Table 5). Therefore, the cold drawing should lead to an increase in the lateral component of the dipole moment of the kinetic unit; that is, μ_{eff} should increase. As follows from Tables 4 and 5, upon orientation, θ is also changed. The appearance of dichroism in the "amorphous" bands (Table 4) attests to the development of a preferential orientation of the segments in the amorphous phase. This observation is also supported by the X-ray diffraction data (see the value of *f*a for film 1 in Table 5). According to expressions (2) and (3), this trend implies that a decrease in the disordered orientation angle of kinetic segments upon cold drawing should also provide its contribution to the above increase in the intensity of the α_a-process.

Table 2. Some characteristics of isotropic films 1 and 2

Sample, N	*p*, g/cm^3	Speed of sound, m/s	E, Gpa	L^{001}, nm	D/d, cm^{-1}		
					880	1075	1177
1	1.805	1410	3.60	4.9	1237	250	1620
2	1.805	1300	2.36	5.0	785	157	1000

Table 3. Normalized optical densities of conformationally sensitive IR bands in isotropic samples 1 and 2

IR bands, cm–1	Phase state	Conformation	*D*/*d*, cm^{-1}	
			sample 1	sample 2
470	Amorphous	TT	225	250
490	"	TG	172	195
510	Amorphous, crystalline	TT	180	202
600	Amorphous	-	19	50
813	-	$T_3GT_3G^-$	100	68
840	-	$(-TT-)_n$ $n >$ 3	500	383
1235	Crystalline	$T_3GT_3G^-$	900	613
1275	-	$(-TT-)_n$ $n >$ 4	580	613

Table 4. Spectral characteristics of oriented samples 1 and 2

IR band,cm^{-1}	Parameter	Conformation	Phase state	Sample 1`	Sample 2
470	D/d, cm^{-1}	TT	Amorphous	393	225
	R			17	5
490	D/d, cm^{-1}	TG	Amorphous	486	490
	R			1.8	0.8
510	D/d, cm^{-1}	TT	Amorphous, Crystalline	977	428
	R			3.4	2.6

Table 5. Structural characteristics of the oriented films of the VDF–TFE copolymer with different initial morphology

Sample	L, nm	l_a, nm	l_a, nm	$l_{110,200}$, nm	$\Delta\phi_{001}$, deg	f_c	$\Delta\phi_a$, deg	f_a
1	7.8	5.9	1.9	6.6	20	0.82	41	0.35
2	-	6.0	-	7.0	11	0.94	49	0.15

Comparing the dependences Δε(T) for both oriented films (curves 1', 2' in Fig. 3), one may conclude that, in the region of the α_a-dispersion, the Δε of film 1 appears to be almost three times higher than that of film 2. If one assumes that a certain fraction of the volume in film 2 is occupied by microcracks, the concentration of dipoles decreases by only a factor of 1.5. Therefore, the lower values of Δε for film 2 cannot

be explained solely by the absence of microcracks in the volume of the sample. According to formula (2), additional factors responsible for the intensity of relaxation processes are provided by the fractional content of the disordered phase and the state of its chain orientation. The analysis of the variations in the intensities of "amorphous" bands (Tables 3, 4) shows that, upon cold drawing, the amorphization of film 2 proceeds to a lesser extent than that of film 1. This conclusion is also proved by the acoustic data (compare curves 2, 3); that is, in the oriented film 2, the concentration of kinetic units responsible for the α_a-relaxation should be lower than that in film 1. According to expression (2), this serves as an additional factor providing a decrease in $\Delta\varepsilon$. For film 2, the μ_{eff} values as expressed through the above kinetic units should also be lower because the concentration of trans-isomers in its amorphous phase is reduced (c.f. the bands at 470 and 510 cm^{-1} in Table 4 for both films).

According to relationship (2), one should also compare the mean angles of disordered orientation of the kinetic units in both oriented films. These values may be evaluated from the dichroic ratio R of "amorphous" bands. As follows from Table 4, in the case of film 2, the above values are higher than those of film 1. This conclusion is also supported by the data of X-ray analysis, where the mean angle of disordered orientation $\Delta\phi_a$ is estimated through the azimuthal scanning of an amorphous halo in the equatorial direction. As follows from Table 5, for film 2, $\Delta\phi_a$ is higher than that in film 1. Therefore, the lower values of $\Delta\varepsilon$, as observed for the oriented film 2 in the glass transition region, should be related to the three following reasons: a decrease in the concentration of dipoles upon the development of microcracks, a lower degree of "amorphization" of the isotropic film upon its cold drawing, and a higher disorder of the kinetic segments in the amorphous phase with a lower effective dipole moment.

Table 5 demonstrates that the above oriented films show quite different characteristics of the crystal reorientation, which are estimated by the azimuthal scanning of the X-ray reflection (001). As is seen, at the same longitudinal and lateral sizes of crystals, their disordered orientation angles $\Delta\phi_{001}$ differ by almost two times. Hence, the development of microcracks upon cold drawing favors the development of a more perfect orientation of the crystals. This conclusion qualitatively agrees with the data on the mechanism of the development of microcracks in PE reported in [3]. This observation may also concern the character of variations in the relaxation times of the α_a-process upon cold drawing of film 2. As is known, within the model of free volume *f*, the mean frequencies of disordered orientation $\nu \sim f$. This implies that, for the oriented sample 2 containing microcracks, that is, the regions with a reduced density, one should anticipate a shift in the relaxation α_a-transition to lower temperatures (compared with the isotropic sample). As is seen, Figs. 1 and 2 suggest quite the reverse behavior. Therefore, the "free volume" developed by microcracks does not restrict the temperature corresponding to the onset of cooperative mobility in the disordered phase. The reason for this trend is that an increased orientation of crystals upon cold drawing of film 2 may lead to the formation of a certain fraction of stressed chains in the amorphous phase. Such chains are characterized by a reduced conformational entropy and should be localized in the vicinity of oriented crystals, that is, in interphase regions. The mobility responsible for the α_a-β.-process in such regions is activated [12, 16]; hence, the increased values of entropy and enthalpy observed in this dispersion region upon cold drawing of sample 2 (Table 1) prove the above speculations.

Another aspect of this problem is related to the development of the ferroelectric state in the copolymers studied. The mechanism of this phenomenon is still unclear [6]. The analysis shows that one of the fundamental characteristics of ferroelectrics, such as the residual polarization P_r, appears to be higher in oriented films than in isotropic samples [6]. In this connection, the preparation of films based on the above materials with an increased level of P_r is quite a demanding task [27, 28]. Below, for film 1, we will consider the effect of cold drawing on the level of residual polarization.

Figure 8 presents the curves of electric hysteresis for the isotropic and oriented film 1. As is seen, in the latter case, the values of the maximum and residual polarizations appear to be several times higher. A similar behavior was observed in [16] for cold-drawn films of the same copolymer but with different morphology of the isotropic samples.

ISSN: 0975-8585

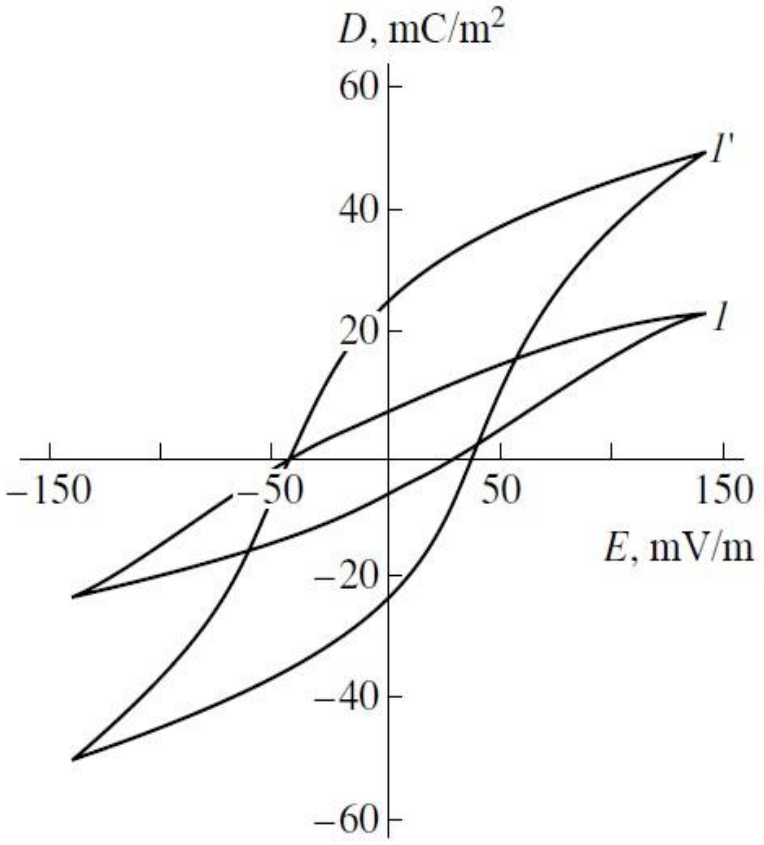

Fig. 8. Dielectric hysteresis curves for (*1*) isotropic and (*1*') cold-drawn films of the VDF–TFE copolymer

When the field is applied, the polar crystals with dipole moment M_c begin to orient along its direction. At a given voltage, the equilibrium position M_{ci} is characterized by a certain distribution function for the polar axes of crystals relative to the normal [6]. This is similar to the introduction of a certain averaged angle γ between the direction of the applied field and the polar axis of the crystal. In this case, the expression for P_r should take the following form:

$$P_r = \frac{N \sum_i M_{ci}}{V} \langle \cos\gamma \rangle , \qquad (4)$$

where V is the volume of the sample containing N crystals. Using expression (4), one may speculate on the reasons for the marked increase in P_r upon the orientation of film 1. When the general relationships are presented in the Cartesian coordinates [24], ‹cos γ›. ~ ‹cos θ›. For an isotropic film, ‹cos θ›. = 0.57, but, as follows from relationship (3) and Table 5, upon orientation, ‹cos θ› = 0.98. As is seen in Fig. 8, the difference between P_r for both films may be as high as 300%.

Therefore, the above difference cannot be explained solely by the orientational phenomena. As was shown above, upon cold drawing, film 1 experiences a noticeable amorphization. If the principal contribution to P_r is assumed to be provided by polar crystals [6], then, according to relationship (4), due to the above factor, one should expect a decrease in the residual polarization upon cold drawing; however, quite the reverse situation is observed. This disagreement may be explained by the different character of the dynamics of both films. At the temperature of polarization (20°C), the molecular mobility in films 1 is characterized by the presence of a α_a-β -relaxation region. As follows from Table 1, in this dispersion region, all activation parameters in the oriented film appear to be lower than those in the isotropic film. Within the framework of the fluctuation model advanced for the development of nucleation sites of new domains in interphase regions

[6], the character of chain dynamics should affect the resultant level of residual polarization. Low activation parameters of the α_a-β -dispersion in the above interphase boundaries should increase the probability of the nucleation of domains with a new direction. At the same time, upon polarization, an increased mobility of polymer chains in the boundary regions of crystals may enhance field-induced phase transformations [1]. This may concern the transitions of an anisotropic amorphous phase to a polar crystal, which may assist an increase in the degree of crystallinity, as has been observed experimentally [1, 6].

CONCLUSION

As was mentioned above [1, 6], in the systems studied, well before the Curie transition, ferroelectric crystals may coexist with crystals with different types of packing. Such crystals manifest themselves as the X-ray reflection halo at 2θ ~ 18° [12]. This X-ray reflection is associated with either a paraelectric or antiferroelectric phase. One of the typical features of the latter phase concerns the presence of double loops in the corresponding dielectric hysteresis curves. The appearance of such loops has been observed for VDF–trifluroethylene copolymers [6, 29, 30], as well as for VDF.TFE copolymers [31, 32] of the same composition as studied in this work. In this connection, the presence of an antiferroelectric phase in the films studied seems to be quite verisimilar. In the polarization under an applied field with a frequency of 50 Hz, double loops of hysteresis are seen only at low intensities [31, 32]. At a high field and a low frequency of its sweep (10^{-2}–10^{-3} Hz), they appear only in the first several cycles [29]; after that, their transformation into a single loop is seen. The above observation suggests that the antiferroelectric phase is metastable, and, under the action of a field with an increased intensity, this phase is transformed into a ferroelectric phase. This process may serve as an additional factor promoting an increase in both the maximum and residual polarization in a cold-drawn film.

For the oriented film of the copolymer studied, the effect of microcracks on the ferroelectric properties was earlier discussed in [7]. According to expression (4), as the number of polar crystals in the matrix is decreased, the residual polarization should be reduced. This trend was observed experimentally [7]. As a result of the isometric annealing [7], an increase in P_r may be related to an increase in N due to the "healing" of a certain fraction of microcracks, as well as due to a concomitant increase in the degree of crystallinity [33].

ACKNOWLEDGMENTS

The article was prepared within the framework of the Federal Target Program (FTP) «Research and development on priority directions of development of scientific-technological complex of Russia for 2014-2020». The number of Agreements for the provision of grants: 14.576.21.0029, the unique project code: RFMEFI57614X0029.

REFERENCES

[1] Kochervinskij, V.V., Sokotov, V.G., Zubkov, V.M. Effect of the molecular structure on characteristics of electrical hysteresis of polyvinylidene fluoride and its copolymers (1991) Vysokomolekularnye Soedineniya. Seriya A, 33 (3), pp. 530-537.

[2] Periasamy, P., Tatsumi, K., Shikano, M., Fujieda, T., Sakai, T., Saito, Y., Mizuhata, M., Kajinami, A., Deki, S. An electrochemical investigation on polyvinylidene fluoride-based gel polymer electrolytes (1999) Solid State Ionics, 126 (3-4), pp. 285-292.

[3] Takahashi, Y., Kodama, H., Nakamura, M., Furukawa, T., Date, M. Antiferroelectric-like behavior of vinylidene fluoride/trifluoroethylene copolymers with low vinylidene fluoride content (1999) Polymer Journal, 31 (3), pp. 263-267.

[4] Eberle, G., Schmidt, H., Eisenmenger, W. Piezoelectric polymer electrets (1996) IEEE Transactions on Dielectrics and Electrical Insulation, 3 (5), pp. 624-646.

[5] Nogales, A., Ezquerra, T.A., García, J.M., Baltá-Calleja, F.J. Structure-dynamics relationships of the α-relaxation in flexible copolyesters during crystallization as revealed by real-time methods (1999) Journal of Polymer Science, Part B: Polymer Physics, 37 (1), pp. 37-49.

[6] Kochervinskij, V.V. The effect of radiation on ferroelectric characteristics of poly(vinylidene fluoride) (1993) Vysokomolekularnye Soedineniya. Ser.A Ser.B Ser.C - Kratkie Soobshcheniya, 35 (12), pp. 1978-1985.

[7] Kochervinskii, V.V. The properties and applications of fluorine-containing polymer films with piezo- and pyro-activity (1994) Russian Chemical Reviews, 63 (4), pp. 367-371.
[8] Bharti, V., Xu, H.S., Shanthi, G., Zhang, Q.M., Liang, K. Polarization and structural properties of high-energy electron irradiated poly(vinylidene fluoride-trifluoroethylene) copolymer films (2000) Journal of Applied Physics, 87 (1), pp. 452-461.
[9] Kochervinskii, V.V. Electrophysical properties of ultrathin films of ferroelectric polymers (2005) Polymer Science - Series B, 47 (3-4), pp. 75-103.
[10] Kochervinskiĭ, V.V. Structural changes in ferroelectric polymers under the action of strong electric fields by the example of polyvinylidene fluoride (2006) Crystallography Reports, 51 (SUPPL. 1), pp. S88-S107.
[11] Kochervinskii, V.V. Mechanism of polarization and piezoelectric behavior in crystallizable ferroelectric polymers from the standpoint of propagation of soliton waves (2006) Polymer Science - Series C, 48 (1), pp. 38-57.
[12] Kochervinskii, V., Malyshkina, I., Gavrilova, N., Sulyanov, S., Bessonova, N. Peculiarities of dielectric relaxation in poly(vinylidene fluoride) with different thermal history (2007) Journal of Non-Crystalline Solids, 353 (47-51), pp. 4443-4447.
[13] Despotopoulou, M., Burchill, M.T. Coatings for electrochemical applications (2002) Progress in Organic Coatings, 45 (2-3), pp. 119-126.
[14] Wagner, A., Kliem, H. Dispersive ionic space charge relaxation in solid polymer electrolytes. I. Experimental system polyethylene oxide (2002) Journal of Applied Physics, 91 (10 I), pp. 6630-6637.
[15] Saikia, D., Han, C.C., Chen-Yang, Y.W. Influence of polymer concentration and dyes on photovoltaic performance of dye-sensitized solar cell with P(VdF-HFP)-based gel polymer electrolyte (2008) Journal of Power Sources, 185 (1), pp. 570-576.
[16] Kochervinskii, V.V., Malyshkina, I.A., Markin, G.V., Gavrilova, N.D., Bessonova, N.P. Dielectric relaxation in vinylidene fluorideHexafluoropropylene copolymers (2007) Journal of Applied Polymer Science, 105 (3), pp. 1101-1117.
[17] Neese, B., Chu, B., Lu, S.-G., Wang, Y., Furman, E., Zhang, Q.M. Large electrocaloric effect in ferroelectric polymers near room temperature (2008) Science, 321 (5890), pp. 821-823.
[18] Kochervinskii, V.V., Kozlova, N.V., Khnykov, A.Y., Shcherbina, M.A., Sulyanov, S.N., Dembo, K.A. Features of structure formation and electrophysical properties of poly(vinylidene fluoride) crystalline ferroelectric polymers (2010) Journal of Applied Polymer Science, 116 (2), pp. 695-707.
[19] Kochervinskii, V., Malyshkina, I. Peculiarities of high-temperature dielectric relaxation in vinylidene fluoride - hexafluoropropylene copolymers (2010) Journal of Non-Crystalline Solids, 356 (11-17), pp. 564-567.
[20] Kochervinskii, V.V. (2009) Proceedings of All-Russia Conference "physicochemical Aspects of Technology of Nanomaterials, Their Properties and Application", p. 58.
[21] Asadi, K., De Leeuw, D.M., De Boer, B., Blom, P.W.M. Organic non-volatile memories from ferroelectric phase-separated blends (2008) Nature Materials, 7 (7), pp. 547-550.
[22] Dowben, P.A., Rosa, L.G., Ilie, C.C., Xiao, J. Adsorbate/absorbate interactions with organic ferroelectric polymers (2009) Journal of Electron Spectroscopy and Related Phenomena, 174 (1-3), pp. 10-21.
[23] Taguet, A., Ameduri, B., Boutevin, B. Crosslinking of vinylidene fluoride-containing fluoropolymers (2005) Advances in Polymer Science, 184, pp. 127-211.
[24] Neidhöfer, M., Beaume, F., Ibos, L., Bernès, A., Lacabanne, C. Structural evolution of PVDF during storage or annealing (2004) Polymer, 45 (5), pp. 1679-1688.
[25] Emmert, S., Wolf, M., Gulich, R., Krohns, S., Kastner, S., Lunkenheimer, P., Loidl, A. Electrode polarization effects in broadband dielectric spectroscopy (2011) European Physical Journal B, 83 (2), pp. 157-165.
[26] Li, L., Twum, E.B., Li, X., McCord, E.F., Fox, P.A., Lyons, D.F., Rinaldi, P.L. 2D-NMR characterization of sequence distributions in the backbone of poly(vinylidene fluoride-co -tetrafluoroethylene) (2012) Macromolecules, 45 (24), pp. 9682-9696.
[27] Von Seggern, H., Fedosov, S. Conductivity induced polarization in a semicrystalline ferroelectric polymer (2004) IEEE Transactions on Dielectrics and Electrical Insulation, 11 (2), pp. 232-241.
[28] Kochervinskii, V.V., Kiselev, D.A., Malinkovich, M.D., Pavlov, A.S., Kozlova, N.V., Shmakova, N.A. Effect of the structure of a ferroelectric vinylidene fluoride- tetrafluoroethylene copolymer on the characteristics of a local piezoelectric response (2014) Polymer Science - Series A, 56 (1), pp. 48-62.

[29] Yuan, Y., Reece, T.J., Sharma, P., Poddar, S., Ducharme, S., Gruverman, A., Yang, Y., Huang, J. Efficiency enhancement in organic solar cells with ferroelectric polymers (2011) Nature Materials, 10 (4), pp. 296-302.

[30] Xia, W., Xu, Z., Zhang, Z., Li, H. Dielectric, piezoelectric and ferroelectric properties of a poly (vinylidene fluoride-co-trifluoroethylene) synthesized via a hydrogenation process (2013) Polymer (United Kingdom), 54 (1), pp. 440-446.

[31] Kochervinskii, V.V., Chubunova, E.V., Lebedinskii, Yu., Shmakova, N.A. Effect of electrode material on contact high-voltage polarization in a vinylidene fluoride-hexafluoropropylene copolymer (2011) Polymer Science - Series A, 53 (10), pp. 912-928.

[32] Kochervinskii, V.V., Chubunova, E.V., Lebedinskii, Yu., Shmakova, N.A., Khnykov, A.Yu. The role of new functional groups in the surface layer of LDPE during its high-voltage contact polarization (2011) Polymer Science - Series A, 53 (10), pp. 929-946.

[33] Kochervinskii, V., Malyshkina, I., Pavlov, A., Bessonova, N., Korlyukov, A., Volkov, V., Kozlova, N., Shmakova, N. Influence of parameters of molecular mobility on formation of structure in ferroelectric vinylidene fluoride copolymers (2015) Journal of Applied Physics, 117 (21), art. no. 214101.